UNIVERSIDAD DISTRITAL
FRANCISCO JOSÉ DE CALDAS

Ingeniería

https://revistas.udistrital.edu.co/index.php/reving/issue/view/1320

DOI: https://doi.org/10.14483/23448393.23090

Research

Assessing the Efficacy of optimization algorithms, P&O and MPC in MPPT for Photovoltaic Systems: A Comparative Study

Evaluación de la eficacia de los algoritmos de optimización, P&O y MPC en MPPT para sistemas fotovoltaicos: Un estudio comparativo

Jose Mena-Palomeque[1], Juan E. Zabala-Daza[2], Jhon A. Gómez P.[1], Jaime A. Ramírez-Ospina[1]

[1]IU Digital, Medellín, Colombia
[2]ITM, Medellín, Colombia

Abstract

Context: The need for efficient energy harvesting in photovoltaic (PV) systems requires advanced maximum power point tracking (MPPT) techniques. Traditional methods like perturb and observe (P&O) exhibit limitations under varying conditions, leading to less efficient energy extraction.
Method: This study compares a model-predictive controller (MPC) combined with optimization algorithms such as the particle swarm optimizer (PSO), the vortex search algorithm (VSA), and the salp swarm algorithm (SSA) to improve MPPT performance in PV systems. These algorithms are tested under different irradiance conditions to assess their efficiency and adaptability.
Results: The results show that PSO, when used with MPC, greatly enhances energy extraction compared to the conventional P&O method. Additionally, VSA and SSA also perform well in adapting to rapid irradiance changes, ensuring an optimal power output.
Conclusions: Optimization-based MPPT methods, especially those using PSO, offer significant efficiency improvements for PV systems, making them strong alternatives to traditional techniques.
Keywords: Solar Power System, Partial Shading, PS, PV, Power Converter, MPPT, MPC, Optimization Algorithms, Energy Efficiency.

Article history

Received:
26th/February/2025

Modified:
10th/December/2025

Accepted:
3th/February/2026

Ing, vol. 31, no. 1, 2026. e23090

*Correspondence: Jose.mena@prof.iudigital.edu.co

Resumen

Contexto: La creciente demanda de extracción eficiente de energía en sistemas fotovoltaicos (PV) requiere técnicas avanzadas de seguimiento del punto de máxima potencia (MPPT). Métodos tradicionales como *perturb and observe* (P&O) enfrentan limitaciones bajo condiciones ambientales variables, conlleva una extracción subóptima de energía.
Método: Este estudio presenta un análisis comparativo de un controlador predictivo de modelos (MPC) integrado con varios algoritmos de optimización, incluyendo la optimización por enjambre de partículas (PSO), el algoritmo de búsqueda de vórtices (VSA) y el algoritmo de enjambre de salpas (SSA), para mejorar el rendimiento del MPPT en sistemas PV. Los algoritmos fueron evaluados bajo diferentes perfiles de irradiancia para determinar su eficiencia y adaptabilidad.
Resultados: Los resultados indican que PSO, cuando se combina con MPC, mejora significativamente la eficiencia de extracción de energía en comparación con el método convencional P&O. Además, VSA y SSA también demuestran un rendimiento superior al adaptarse a cambios rápidos en la irradiancia, asegurando una salida de potencia óptima.
Conclusiones: Los métodos MPPT basados en optimización, particularmente aquellos que utilizan PSO, ofrecen mejoras sustanciales en la eficiencia de los sistemas PV, lo que los posiciona como alternativas viables a las técnicas MPPT tradicionales.

Palabras clave: Sistema de energía solar, Sombreado parcial, PS, PV, Convertidor de potencia, MPPT, MPC, Algoritmos de Optimización, P&O, Eficiencia Energética.

1. Introduction

The rapid rise in global population density has significantly increased the demand for energy, food, and natural resources (1). Fossil fuels, including oil, coal, and natural gas, are the world's primary energy sources (2–4), but its reliance on them raises concerns about depletion and environmental impact (5). In response, renewable energy has become pivotal in the global transition (6).

Photovoltaic (PV) systems stand out as a promising alternative since they convert solar energy into electricity. With components like power converters, PV panels, and electrical loads, they require coordination to operate efficiently (7, 8). Bypass diodes protect PV panels from reverse currents, preventing shading effects that reduce efficiency and lifespan (9).

PV systems use DC/DC and DC/AC converters to adapt to load needs (10), monitoring current and voltage for optimal energy management (11). Maximum power point tracking (MPPT) strategies maximize energy extraction by adapting to environmental variations (12), adjusting the output voltage to optimize conversion efficiency (13).

MPPT techniques include approaches based on P&O (14), incremental conductance (INC) (15, 16), MPPT-current (MPPT-I) (17), MPPT-voltage (MPPT-V) (18), neural networks (19), and genetic algorithms (20–22). Still, some challenges remain in achieving precise, rapid MPPT adaptation to environmental changes, with methods like P&O often leading to oscillations under fluctuating irradiance (23, 24). Complex controllers must respond to shading conditions (25), though the high costs of advanced methods and hardware pose barriers (13). Thus, PV systems require DC/DC or DC/AC converters

to consistently supply energy to loads, ensuring efficiency across operating conditions (26).

1.1. State of the art

The specialized literature presents numerous studies on the MPPT search problem regarding PV panels, highlighting the widespread use of the P&O algorithm, often combined with proportional-integral-derivative (PID) controllers, model-predictive control (MPC), sliding mode control, and more. This study focuses on validating and comparing various MPPT algorithms with MPC controllers, in order to identify the approach that maximizes power extraction under variable irradiance scenarios.

The MPPT problem has been widely solved in the specialized literature (14,15,27–33), using methods based on artificial intelligence (AI), such as neural networks (NNs), genetic algorithms (GAs), and fuzzy logic to improve efficiency and accuracy under different environmental and irradiance conditions. In addition, hybrid techniques have been developed which combine multiple algorithms to obtain a more robust and accurate response to different operational contexts.

In (30), the authors review MPPT algorithms, classifying them by key performance indicators to aid the selection of suitable algorithms for PV systems. This study highlights challenges in control strategies, including poor performance under partial shading, steady-state oscillations, slow convergence, implementation complexity, and limited use of real data or experiments.

The work by (14) introduces SOFT-MPPT, an MPPT algorithm for P&O-based PV systems that employs an adaptive modulation factor to correlate PV current measurements with irradiance, aiming to enhance energy extraction efficiency. Although the authors claim high efficiency, their study lacks data to fully substantiate these assertions. The proposed comparative analysis of MPPT techniques does not quantitatively validate the algorithm's performance in terms of maximum power or point tracking accuracy. Furthermore, no comparisons with standard MPPT strategies are provided, nor is the algorithm tested under variable weather or partial shading conditions.

The study by (15) proposes a control algorithm that combines unit vector template (UVT) and power balance theory (PBT) for a PV system implementing an MPPT strategy to enhance power stability. Although an appropriate evaluation of the MPPT strategy is conducted, the authors do not perform a comparative analysis with other MPPT methods, making it challenging to assess the efficiency of the proposed solution for time-varying systems. Additionally, while the authors assert that the solution's performance was evaluated in terms of DC voltage regulation quality and mains current harmonic mitigation under linear and nonlinear load conditions, no results or data supporting these claims are provided, limiting the proper validation of the study's findings.

In (27), an MPPT strategy based on the Mayfly optimization algorithm for PV systems under variable conditions is proposed. The authors test the approach in Matlab/Simulink, comparing it to the PSO algorithm. However, limitations arise since evidence for MPPT success under dynamic conditions is insufficient, with no demonstration of irradiance variation or a direct comparison of power output between methods. Additionally, details on convergence to the MPPT voltage reference are unclear, necessitating further evaluation to clarify algorithm performance and confirm the authors' claims.

The authors of (28) propose a fuzzy logic-based driver coupled with an MPPT algorithm inspired by the IFFO (*i.e.*, farmland fertility method), aiming to optimize PV system controller parameters under different climate scenarios, achieving over 99 % efficiency in both uniform irradiation (UI) and power

supply (PS) contexts. However, limitations arise from the lack of discussion on the method's constraints and the algorithm's performance under variable conditions. Additionally, the power curves do not fully capture energy fluctuations, and there is minimal information on voltage reference points within the MPPT process, raising questions about the method's applicability across varying PV generation profiles and its reproducibility in achieving stated efficiencies.

In (29), the authors propose a reinforcement deep learning-based MPPT control for PV systems under partial shading conditions. They use deep reinforcement learning (DRL) algorithms, specifically Deep Q-Network (DQN) and Deep Deterministic Policy Gradient (DDPG), to optimize the MPPT control strategy. This approach is compared against the conventional P&O method and evidences higher energy production as well as better tracking performance, especially in scenarios where global MPPT cannot be obtained. However, the authors do not provide information on the statistical validations used to ensure that the experiment performed is repeatable and applicable to other PV panel curves, which does not allow scaling the implementation to other test cases.

The work by (31) presents a fuzzy logic-based controller that integrates the grey wolf optimizer (GWO) into its MPPT strategy to enhance energy extraction in PV systems. The authors employ opposition-based learning (BLO) to accelerate the search for the optimal solution and simulate partial shading conditions to better reflect real-world scenarios. However, this article lacks detailed results—including specific data, graphs, or tables—to support the effectiveness of the proposed method. Additionally, it does not provide comparative analyses with existing methods or discuss potential limitations, necessitating further evidence to substantiate its claims.

In (32), the authors propose a fuzzy logic-based controller that incorporates the GWO within its MPPT strategy to enhance energy extraction in PV systems. They use the BLO method to expedite the search for the optimal solution. Additionally, they suggest a PV energy conversion system using a boost converter and digital filtering within the controller to improve signal quality, optimizing MPPT through the P&O algorithm. However, this article lacks clarity with regard to its methodology, making replication and validation challenging. Although experimental results are mentioned, specific numerical values and procedural details are absent. The study also omits comparisons with other MPPT techniques and does not use statistical tests to validate solution quality, which could impact result interpretation and generalizability.

The authors of (33) authors propose an MPPT method that uses system identification (SI) with an adaptive reference voltage (AVR) and a proportional-integral (PI) controller while incorporating a polynomial model. This approach, designed for simplicity, is compared against MPPT techniques such as P&O, IC, CVR, ANN, and a nonlinear AVR-SI method. However, the study lacks in-depth descriptions of these MPPT strategies, statistical analyses, and a discussion of the limitations.

Additionally, variable climatic conditions affecting PV generation and the lack of comparative analyses between algorithms highlight gaps in existing research. To address these gaps, our study proposes a methodology for comparing various MPPT algorithms via a cost function to characterize MPC within a PV system with a boost converter and a battery. The aim is to identify the algorithm that optimally extracts power under varying irradiance. For comparison, P&O and optimization algorithms, *i.e.*, the particle swarm optimizer (PSO), the vortex search algorithm (VSA), and the salp swarm algorithm (SSA), are considered.

Our choice of PSO, VSA, and SSA was supported by recent literature on PV MPPT, where optimization and swarm-based techniques are widely used to improve efficiency and energy extraction under varying and partial shading conditions. In particular, the use of the SSA for MPPT to optimize the duty cycle of a DC/DC converter and maximize power extraction has been reported, demonstrating the applicability of bio-inspired optimization techniques in PV systems (34). Likewise, hybrid and metaheuristic optimization methods that combine swarm intelligence with conventional MPPT strategies have been shown to enhance tracking performance when compared to traditional techniques (35).

1.2. Scope and main contributions

This study compares different MPPT algorithms implemented in a DC/DC boost converter connected to a PV panel and a battery using an MPC controller with the aim of achieving maximum power extraction. Strategies such as P&O, PSO, VSA, and SSA are used, evaluating an objective function with respect to the voltage of the system.

The main contributions in this study are presented below.

- The development of a comparison methodology between different optimization algorithms in order to achieve maximum power extraction.
- The simulation of variable irradiance conditions for a PV panel within a 24-hour scenario.
- A comparison between the results obtained with the P&O algorithm and those of other optimization techniques widely used in the specialized literature, including PSO, VSA, and SSA. This comparison is based on the maximum power extraction of the system and how these algorithms reach the desired benchmarks, implementing irradiance scenarios on an average day and critical irradiance cases.
- The implementation of an MPC controller for a PV system comprising a DC/DC converter and a battery while using optimization algorithms, in order to compare the results in terms of maximum energy extraction.

  To summarize, this article presents an approach for MPP tracking using an MPC controller within a PV system linked to a boost converter and a battery. Two irradiance scenarios are considered: an average day and a fluctuating day under critical conditions. This study compares the P&O algorithm against PSO, VSA, and SSA to determine the most effective method for maximizing energy extraction through MPPT.

1.3. Structure of the paper

This paper is organized as follows. Section 2 details the mathematical formulation, circuit diagrams, technical specifications, and MPC controller configuration. Section 3 describes the algorithms and the objective function for MPPT. Section 4 covers the simulation stage, experimental voltage and current data, and MPC implementation in Matlab, including the representation of maximum energy extraction. The results of each algorithm are analyzed in terms of energy extraction percentage by integrating areas under power curves. Finally, Section 5 presents the main conclusions of our work.

2. Mathematical Formulation

This section presents the mathematical modeling for the PV system and the boost DC/DC converter connected to a battery. The MPC controller with the MPPT algorithms (P&O, PSO, SSA, and VSA) is implemented on these models. All of this is done with the objective of tracking the maximum power point and validating which algorithm enables the highest power transfer.

2.1. Mathematical model of the PV panel

A PV panel converts solar radiation into electrical energy via p-n junction semiconductors, with its power output varying according to solar irradiance and ambient temperature. This variability can be accurately modeled using the single-diode model (SDM), as shown in Eq. (1), which is highly valued for both accuracy and simplicity. Additionally, the PV panel can be represented by an equivalent circuit comprising a current source in parallel with a diode and two resistors connected in parallel and series (Fig. **1**).

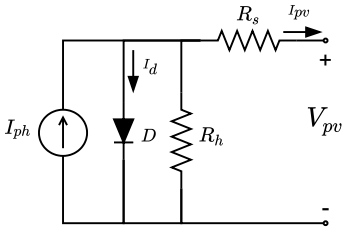

Figure 1. Equivalent circuit for the SDM

$$I_{pv} = I_{ph} - I_d \left[e^{\left(\frac{V_{pv} + R_s I_{pv}}{\eta \frac{N_s kT}{q}} \right)} - 1 \right] - \left(\frac{V_{pv} + R_s I_{pv}}{R_h} \right) \tag{1}$$

Eq. (1) represents the output current of the panel I_{pv}, the photo-induced current I_{ph}, the reverse saturation current of the diode I_d, the electron charge q, the output voltage V_{pv}, the ideality factor η_1, the Boltzmann constant k, and the panel temperature T.

$$I_{ph} = \left(\frac{G}{G_{ref}} \right) \cdot (I_{ph,ref} + \mu \cdot (T_c - T_{ref})) \tag{2}$$

Although Eq. (2) is a simplified model adapted for use cases and modeling involving power converters, I_{ph} is proportional to the solar irradiance G, which is given in Watts per square meter (W/m^2). The term G/G_{ref} represents the ratio between the current irradiance and a reference irradiance G_{ref}, which is generally $1000\ W/m^2$ under standard conditions. $\mu \cdot (T_c - T_{ref})$ accounts for the effect of temperature on the current generated by the panel. Here, T_c denotes the current temperature of the PV panel, T_{ref} is the reference temperature $(25C)$, and the coefficient μ indicates the variation between the current for each degree of change in the temperature.

By using this equation or the electrical circuit, a representation of the PV profiles under any uniform condition of irradiance and temperature can be obtained. It is necessary to understand that

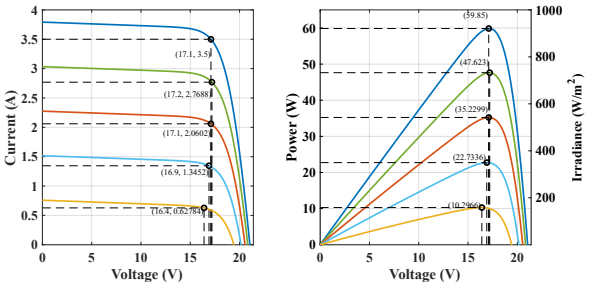

Figure 2. Profile of V_{pv} *vs.* P_{pv} and V_{pv} *vs.* I_{pv} under standard test conditions

the representation of the profiles or the characteristic curves of a PV panel has a maximum power point (MPP), which is determined by the product between the voltage at the maximum point (V_{mpp}) and the current at the maximum point (I_{mpp}). At this point, the highest power is extracted from the panel (P_{mpp}) (Fig. **2**).

2.2. Modeling the PV system for control purposes

To integrate a PV panel, a DC/DC converter, and a battery, it is necessary to establish the effective control point of the converter using pulse-width modulation (PWM). This control focuses on the precise definition of the duty cycles (D), which are constantly adjusted to find the system's optimal operating point. This work typical when dealing with energy generation systems, such as PV panels, which require the constant production of the maximum power point (MPP).

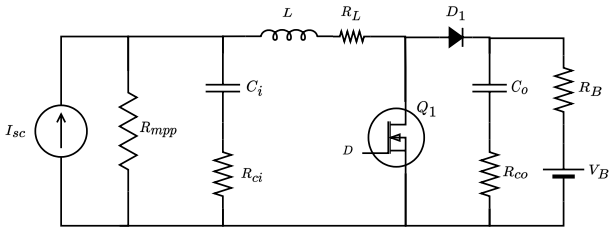

Figure 3. Circuit model for the PV system with converter boost and battery

It should be noted that, in this study, it is necessary to mathematically model the system, which consists of a PV panel, a DC/DC converter, and a battery. To this effect, the PV panel is simplified using the Norton equivalent (Fig. **3**). The current source I_{SC} and the resistance R_{MPP} represent the short-circuit current and the instantaneous impedance of the PV panel. The DC/DC converter is represented by an inductor L and the inductor losses R_L. In addition, R_B denotes the battery resistance, R_{on} is the MOSFET (Q_1) connection resistance, V_f is the diode (D_1) forward voltage, and V_B is the battery's open-circuit voltage. C_i and C_o denote the input and output capacitance of the converter, with their equivalent series resistances R_{ci} and R_{co}, respectively.

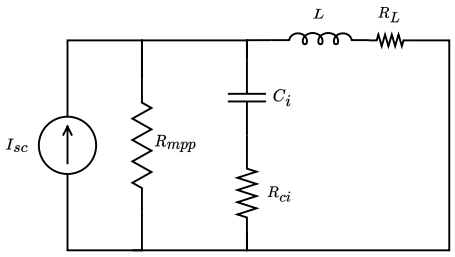

Figure 4. Activation state of the boost converter: Q_1 ON and D_1 OFF

The resulting equations for the state of Q_1 on and D_1 off (Fig. **4**) are determined using Kirchhoff's voltage and current laws, yielding (3)-(6), which represent the currents in the capacitors C_i and C_o, which make up Eqs. (3) and (4), respectively.

$$I_{Ci} = \lambda \cdot I_{SC} - \frac{V_{Ci}}{R_{MPP} + R_{Ci}} \lambda I \tag{3}$$

$$I_{Co} = \frac{V_B}{R_B + R_{Co}} - \frac{V_{Co}}{R_B + R_{Co}} \tag{4}$$

The voltage across the inductor is represented in Eq. (5), where I represents the current flowing through the inductor, V_{Ci} is the voltage across capacitor C_i, and V_{Co} is the voltage across capacitor C_o. Finally, the voltage of the PV panel V_{pv} is obtained via Eq. (6).

$$V_L = \lambda \cdot V_{Ci} + \beta \cdot I_{SC} - (R_L + R_{on} + \beta) \cdot I \tag{5}$$

$$V_{PV} = \lambda \cdot V_{Ci} + \beta \cdot I_{SC} - \beta I \tag{6}$$

On the other hand, to provide a better understanding of the equations mentioned above, it is necessary to expand the parameters λ and β using Eqs. (7) and (8).

$$\lambda = \frac{R_{MPP}}{R_{MPP} + R_{Ci}} \tag{7}$$

$$\beta = \frac{R_{Ci} \cdot R_{MPP}}{R_{MPP} + R_{Ci}} \tag{8}$$

Continuing with the equations for mathematically modeling the converter, the next state of the circuit occurs when Q_1 is off and D_1 is on (Fig. **5**). The resulting equations are (9) and (10).

$$I_{Co} = \theta \cdot I + \frac{V_B}{R_B + R_{Co}} - \frac{V_{Co}}{R_B + R_{Co}} \tag{9}$$

$$V_L = \lambda \cdot V_{Ci} + \beta \cdot I_{SC} - (R_L + \gamma + \beta) \cdot I - V_f - \theta \cdot V_{Co} - \sigma \cdot V_B \tag{10}$$

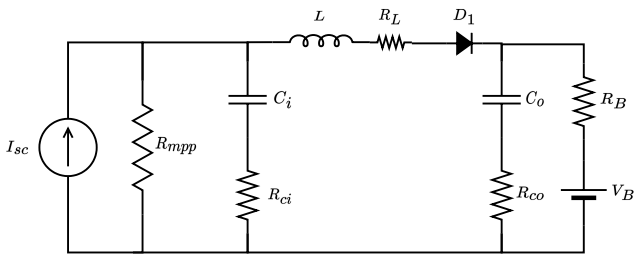

Figure 5. Activation state of the boost converter: Q_1 OFF and D_1 ON

It is worth noting that these equations are a bit lengthy because the entire converter was calculated while considering the losses of each element. This makes the system of equations robust. Therefore, parameters or variables are linked to reduce its size. These parameters are described in Eqs. (11), (12), and (13), which allow for a representation of γ, θ, and σ.

$$\gamma = \frac{R_B \cdot R_{Co}}{R_B + R_{Co}} \tag{11}$$

$$\theta = \frac{R_B}{R_B + R_{Co}} \tag{12}$$

$$\sigma = \frac{R_{Co}}{R_B + R_{Co}} \tag{13}$$

As part of the final system of equations, the system dynamics at any operating point must be defined. For this purpose, a volt-second balance is applied to the inductor, and a charge balance is applied to each capacitor (C_i, C_o). The resulting equations are presented in (14), (15), and (16).

$$\begin{aligned} L\frac{dI}{dt} =& \lambda \cdot V_{Ci} + \beta \cdot I_{SC} - (R_L + d \cdot R_{on} + \beta + (1-d) \cdot \gamma) \cdot I \\ & - (1-d) \cdot V_f - (1-d) \cdot \theta \cdot V_{Co} - (1-d) \cdot \sigma \cdot V_B \end{aligned} \tag{14}$$

$$C_i \frac{dV_{Ci}}{dt} = \lambda \cdot I_{SC} - \frac{V_{Ci}}{\alpha} - \lambda I \tag{15}$$

$$C_o \frac{dV_{Co}}{dt} = (1-d) \cdot \theta \cdot I - \frac{V_{Co}}{\delta} + \frac{V_B}{\delta} \tag{16}$$

Where:

$$\alpha = R_{MPP} + R_{Ci} \tag{17}$$

$$\delta = R_{Co} + R_B \tag{18}$$

Based on the equations that describe the behavior of the system at any operating point throughout the mathematical model, it is possible to implement linear or nonlinear control techniques that allow taking the behavior of the plant to a desired point of operation. This work uses a linear control technique to validate the behavior of the system under different environmental conditions.

In order to apply a linear control technique to the plant, it is necessary to linearize the system at a given operating point. This is adjusted in the equations by applying the Jacobian (36), with the aim of representing all the equations in the state space based on the Characteristic Equations (19) and (20).

$$\dot{X} = AX + BU \tag{19}$$

$$Y = CX + EU \tag{20}$$

Here, X represents the state of the system, U denotes the control inputs, Y signifies the system outputs, and A, B, C, and E are the matrices used to perform the state-space representation of the plant, which is given by Eqs. (21), (22), (23), and (24). It should be noted that the state variables used herein are V_{Ci}, I and V_{Co}. In addition, the input variables are I_{SC} and V_B.

$$X = \begin{bmatrix} V_{Ci} \\ I \\ V_{Co} \end{bmatrix}, \quad U = \begin{bmatrix} I_{SC} \\ V_B \\ d \end{bmatrix}, \quad Y = \begin{bmatrix} V_{pv} \end{bmatrix} \tag{21}$$

$$A = \begin{bmatrix} -\frac{1}{C_i\alpha} & -\frac{\lambda}{C_i} & 0 \\ \frac{\lambda}{L} & -\frac{R_L + \beta + (1-D)\gamma + DR_{on}}{L} & -\frac{(1-D)\theta}{L} \\ 0 & \frac{(1-D)\theta}{C_o} & -\frac{1}{C_o\delta} \end{bmatrix} \tag{22}$$

$$B = \begin{bmatrix} -\frac{\lambda}{C_i} & 0 & 0 \\ \frac{\beta}{L} & -\frac{(1-D)\sigma}{L} & \frac{V_f - (R_{on}-\gamma)I + \sigma V_B + \theta V_{Co}}{L} \\ 0 & \frac{1}{C_o\delta} & \frac{I\theta}{C_o} \end{bmatrix} \tag{23}$$

$$C = \begin{bmatrix} \lambda & -\beta & 0 \end{bmatrix} \tag{24}$$

$$E = \begin{bmatrix} \beta & 0 & 0 \end{bmatrix} \tag{25}$$

Starting from these equations, the implementation and validation of the MPC is carried out. It should be noted that the specifications of the entire system are defined in Table **I**.

2.3. Model-predictive control (MPC)

After defining the mathematical models, MPC can be applied as a modern control technique that uses the system model to predict future behaviors under varying conditions. MPC aims to determine an optimal sequence of control signals that minimizes a cost function over a finite prediction horizon while adhering to input and output constraints (37).

2.3.1. Formulating the optimization problem

At the core of MPC is a quadratic optimization problem solved at each sampling instant, with the purpose of finding the optimal control input sequence that minimizes a quadratic cost function while respecting the system's technical and operational constraints on states, inputs, and outputs.

Table I. Test system parameters and specifications

Parameter	Symbol	Value
Solar Panel Parameters at STC		
Maximum power	P_{mpp}	85 W
Voltage at P_{max}	V_{mpp}	18 V
Current at P_{max}	I_{mpp}	4.72 A
Short-circuit current	I_{SC}	5 A
Open-circuit voltage	V_{OC}	22.1 V
Temperature coefficient of I_{SC}	α_I	0.065 %/°C
Temperature coefficient of the voltage	α_V	-80 mV/°C
Converter Parameters		
Input capacitor	C_i	22 μF
Output capacitor	C_o	22 μF
Inductor	L	330 μH
Inductor resistance	R_L	60 mΩ
ON resistance Mosfet 1	R_{ON1}	35 mΩ
ON resistance Mosfet 2	R_{ON2}	35 mΩ
DC Load Parameters		
DC load equivalent resistance	R_B	60 mΩ
DC load voltage	V_B	24 V

2.3.2. Cost function

The objective function for MPC is defined as $J(U, x(t))$, which consists of the summation of various terms affecting the system, ensuring that, at each time instant, the MPC can solve the problem through quadratic optimization, as shown in Eq. (26).

$$\begin{aligned} J(U, x(t)) = & \sum_{k=0}^{N_p-1} \left(x(k|t) - r(k)\right)^T Q \left(x(k|t) - r(k)\right) \\ & + \Delta u(k|t)^T R \Delta u(k|t) \end{aligned} \tag{26}$$

Here, $x(k+1|t) = Ax(k|t) + Bu(k|t)$ is the predicted state, $u(k|t)$ represents the control input at time instant k, U is the sequence of control inputs to be optimized, Q and R are weighting matrices, N_p is the prediction horizon, N_u is the control horizon, and E and G are matrices defining constraints on states and inputs, respectively. Finally, f_x and f_u represent vectors defining constraints on the states and inputs, respectively. It is worth highlighting that all elements provide the predicted state at time instant k in order to provide information at time instant t.

2.3.3. System constraints

The constraints considered herein prioritize limiting the control signals, states, and outputs of the system, as shown in Eqs. (27) and (28).

- **Input constraints**:

$$Gu(k) \leq f_u \tag{27}$$

- **States constraints**:

$$Ex(k) \leq f_x \tag{28}$$

2.4. Prediction and control horizon

Once the system equations and their restrictions have been defined, it is necessary to determine the parameters of the system.

2.4.1. Prediction horizon

The prediction horizon is defined as N_p and focuses on defining the number of future time steps over which the behavior and progress of the system will be predicted. In other words, the MPC seeks to predict the behavior of the states and outputs of the system over future steps.

2.4.2. Control horizon

In MPC, the control horizon functions similarly to the prediction horizon, with each time step enabling the determination of an optimal control sequence for the next N_u steps. This process iteratively applies optimal inputs, where performance depends on horizon lengths: a shorter horizon limits constraint handling, while a longer one enhances foresight. For the Matlab configuration, see (38). Algorithms like P&O and optimization methods such as PSO, VSA, and SSA are also suggested for effective reference tracking.

3. Maximum Power Point Tracking Algorithms

With an understanding of PV panel behavior, the MPC controller must be considered in relation to the DC/DC converter. The maximum power point (MPP) shifts with changes in irradiance and temperature, necessitating continuous tracking to maintain an optimal energy transfer. To address this issue, we will explore the various algorithms analyzed in this paper.

3.1. Perturb and observe algorithm ($P\&O$)

P&O, one of the most well-known algorithms, is used to maximize energy transmission from a PV panel by continuously tracking the MPP. For a clearer understanding, the reader may consult Figure 1, which depicts the complete flowchart of the P&O algorithm's behavior, detailing how the MPPT is conducted when using this technique.

Algorithm 1 Perturb and observe MPPT algorithm

Data: Initial reference voltage V_{ref}, Step size for voltage perturbation Δ_V, Initial voltage reading V_{prev}, Initial power reading P_{prev}

```
Measure current voltage V  Measure current power P  if P > P_prev then
    if V > V_ref then
        V_ref = V_ref + Δ_V
    end
    else
        V_ref = V_ref − Δ_V
    end
end
else if P < P_prev then
    if V > V_ref then
        V_ref = V_ref − Δ_V
    end
    else
        V_ref = V_ref + Δ_V
    end
end
P_prev = P  V_prev = V  Apply new reference voltage V_ref to the system
```

The process starts by setting the parameter $P(k-1)$, representing the initial voltage change (perturbation), to identify the MPP. The system then reads the voltage $V(k)$ and current $I(k)$ to compute the power $P(k)$ of the PV panel. The P&O algorithm iteratively adjusts the panel's operating voltage by a value dV, either increasing or decreasing it. After each adjustment, the algorithm calculates the resulting power by comparing the new voltage-current product to the previous power $P(k)$. If the power increases, the next adjustment follows the same direction; if it decreases, the direction reverses. This cycle allows P&O to continuously fine-tune the panel's output, ensuring that it consistently operates at peak power despite changing conditions.

3.2. Optimization techniques

Optimization algorithms are commonly used for tracking the MPP through a forward method that stores critical data, including objective function updates and derived individuals. This research compares the P&O algorithm against optimization methods like PSO, SSA, and VSA, in order to determine which one maximizes energy transfer, guiding cost-effective MPPT and MPC combinations.

3.2.1. The particle swarm optimizer (PSO)

The PSO algorithm is a bio-inspired optimization method based on the social behavior of bird flocks and fish schools. It begins by randomly distributing particles throughout the solution space. Each particle then adjusts its position while following an advancement method, as shown in Eq. (29), which depends on its velocity and both personal and swarm experiences.

$$v_i(t+1) = w \cdot v_i(t) + c_1 \cdot r_1 \cdot (p_i - x_i(t)) + c_2 \cdot r_2 \cdot (p_g - x_i(t)) \tag{29}$$

By utilizing each particle's memory and the swarm's collective knowledge, PSO identifies promising candidate solutions. This collective intelligence allows the swarm to converge to an optimal solution, making PSO ideal for engineering problems that require intelligent algorithms and a clear objective function (39).

3.2.2. The vortex search algorithm (VSA)

Inspired by the dynamics of vertically stirred fluids, VSA explores the solution space through Gaussian distributions. With each iteration, the vortex diameter narrows, steering particles toward the most promising solution. VSA's progression relies on calculating the vortex center (μ) and radius (r), with the initial center set by Eq. (30) and the radius adjusted iteratively by Eq. (31).

$$\mu_0 = (x_{\max} + x_{\min})/2 \tag{30}$$

$$r_{t+1} = \sigma_0 \left(1 - \frac{t}{t_{\max}}\right) \epsilon^{-at_{\max}} \tag{31}$$

These equations incorporate the solution search space bounds, the iteration count, and a constant that dictates the radius reduction rate. As the algorithm generates new populations, it evaluates and adjusts individuals based on the solutions obtained, recalibrating the vortex center around the best solution found to ensure a steady convergence to the optimum (40).

3.2.3. The salp swarm algorithm (SSA)

The SSA algorithm, inspired by marine salps moving in chain-like swarms, balances exploration and exploitation by mimicking salp chain dynamics. A leading salp drives exploration, while follower salps focus on local exploitation, adjusting their positions based on the leader's guidance. As the algorithm evaluates the objective function for each salp's position, it continually updates leader and follower roles and positions. This is governed by Eq. (32).

$$X_i\,(t+1) = X_i\,(t) + d \cdot e^{(-\lambda \cdot t)} \cdot \cos\,(2\pi \cdot t) \tag{32}$$

In this equation, $(X_i(t))$ represents the particles' current position, (d) is the distance to the lead salp, and (λ) is a damping parameter. This structure allows the SSA to effectively tackle complex, non-linear, and non-convex optimization problems (41).

Algorithm 2 MPPT using optimization algorithms

Data: Input parameters Vpv and Ipv

Result: The best position $Vmpp = gbest\_position$

begin

Initialize parameters PSO, SSA, VSA **if** *positions is empty* **then**

Initialize random positions within the voltage limits $Vmin$ and $Vmax$ Initialize initial parameters for each algorithm (PSO, VSA, SSA) Set initial $pbest$ values to infinity and positions Set $gbest$ value to infinity and take the first particle position

Compute solar panel power: $Ppv = Vpv \times Ipv$ **for** *particle i in the population* **do**

Compute power for particle using its position and Ipv Adjust the objective function Update the particle's $pbest$ if the new objective function is better Update $gbest$ if the new objective function is better

for *particle i in the population* **do**

Adjust according to the advancement method of each optimization algorithm (PSO, VSA, SSA) Constrain position within voltage limits $Vmin$ and $Vmax$

3.3. Objective function

To track the maximum power point with optimization algorithms, voltage and current readings from the PV panel are essential, as in the P&O method. This is encapsulated in the objective function, where the absolute difference between the particles' computed power and the actual PV panel power is calculated. This is shown in Eq. (33).

$$f(x) = |power - P_{pv}| + |X(i) - V_{ref}| \tag{33}$$

The variable $power$ arises from the product of the particles $(X(i))$ and the current (I_{pv}). It is worth noting that $(X(i))$ represents voltages randomly generated by each of the optimization algorithms, each of which employs distinct advancement methods for individual creation. The actual power of the PV panel, denoted as (P_{pv}), is computed from the PV panel voltage (V_{pv}) and (I_{pv}).

To minimize MPPT calculation error and ensure particle proximity to the reference voltage, the objective function establishes a power-voltage relationship, as shown in Eq. (33). This function reflects the closeness between calculated and actual power, aiming to balance PV power matching with reference voltage tracking for MPPT. The absolute differences in power and voltage are given by $|X(i) - V_{ref}|$.

4. Simulations and results

To validate the process, Matlab/Simulink was used to integrate the DC/DC converter (with losses), the PV panel, and the MPPT controllers, as shown in Fig. **6**. This setup emulated realistic behavior similar to non-ideal physical testing conditions.

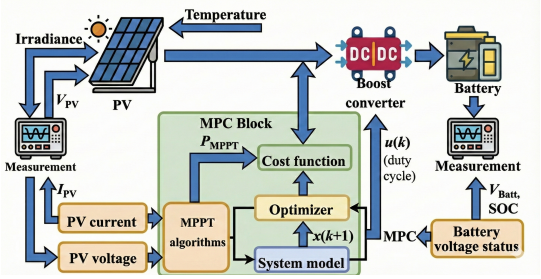

Figure 6. Experimental setup of a Simulink to validate the results

For improved clarity, Fig. **6** explicitly illustrates the interaction between the MPPT algorithm and the MPC controller. The MPPT block generates the PV voltage reference associated with the maximum power point, which is then provided to the MPC controller. The MPC uses this reference to compute the duty cycle required by the DC/DC converter.

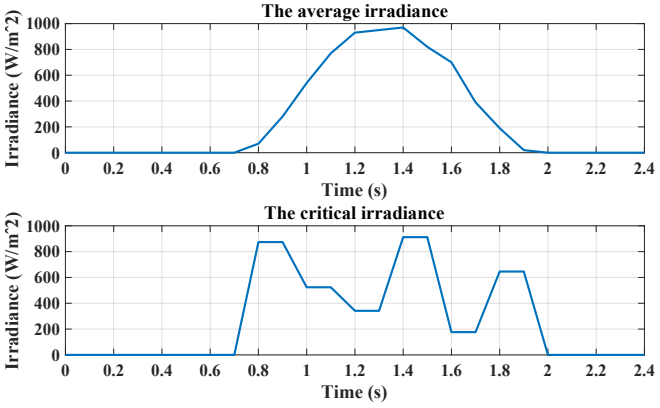

Figure 7. Testing under average and critical conditions

Furthermore, Fig. **7** presents the irradiance profiles to which the controllers and the converter are subjected. It is worth highlighting the inclusion of a critical scenario and an average PV generation curve for the city of Medellín. This is done to validate whether the analyzed optimization algorithms can perform MPPT when using MPC as the controller for the boost DC/DC converter.

4.1. MPC configuration

The MPC is constructed using the state-space representation of the system, as depicted in Eqs. 22 and 23. It is configured using the following parameters:

- Prediction horizon: 2
- Control horizon: 1
- Manipulated variables (MV): Converter's duty cycle (Duty)
- Measured disturbances (MD): Input voltage (V_B) and solar panel current (I_{pv})
- Limits for the manipulated variables:

- MV min: -0.25
- MV max: 0.75

Additionally, to implement the controller in software like Matlab/Simulink, it is essential to incorporate the parameters defined in Table **II**.

Table II. MPC parameters for the boost converter

Parameter	Value
Prediction horizon	2
Control horizon	1
Lower limit of Duty	-0.25
Upper limit of Duty	0.75
Sampling frequency (Ts)	$10e^{-6}$ s

These parameters, set for the controller's use, should be implemented in Matlab code as follows:

```
% System model creation
Boost = ss(A, B, C, D);
% MPC controller configuration
Ts = 10e-6;
% Sampling time
Boost.InputGroup.MV = 3;
% Manipulated variables
Boost.InputGroup.MD = [1 2];
% Measured disturbances
Boost.OutputGroup.MO = 1;
% Manipulated outputs
MPCobj = mpc(Boost, Ts);
% MPC control object
MPCobj.PredictionHorizon = 2;
% Prediction horizon
MPCobj.ControlHorizon = 1;
% Control horizon
MPCobj.ManipulatedVariables.Min = -0.25;
% Lower limit of manipulated variables
MPCobj.ManipulatedVariables.Max = 0.75;
% Upper limit of manipulated variables
```

Listing 1. Configuración del controlador MPC para el convertidor boost.

In the proposed control structure, the MPC is not responsible for reference generation. The voltage reference corresponding to the MPP is generated by the MPPT algorithm. The MPC receives this voltage reference and computes the converter duty cycle (expressed as a percentage) required to drive the PV voltage towards the reference value.

It should be clarified that the MPC controller is designed using a linearized model around an operating point defined by an initial duty cycle $d_0 = 0{,}25$. Therefore, the control input is expressed as a deviation variable $\Delta d = d - d_0$. The limits reported in Table **II** correspond to this deviation variable. When mapped to the physical domain, these limits ensure that the actual duty cycle remains within the feasible range $0 \leq d \leq 1$.

4.2. Test scenarios and considerations

In this section, we analyze the results obtained by the MPC with the optimization algorithms in comparison with the P&O. The aforementioned algorithms were employed in this study to address the challenge of tracking the maximum power point in a PV system. This was achieved using the MPC controller and a boost DC/DC converter while considering critical irradiation and irradiance test scenarios on an average day in the city of Medellín, Colombia. All simulations were conducted in MATLAB $R2023a$ ® on a Dell Precision Tower 5810 workstation equipped with an Intel(R) Xeon(R) CPU E5-1660 v3 @ 3.00GHz, 16 GB of RAM, a 480-GB SSD, and Windows 10.

4.3. Tests under critical operating conditions

One of the primary objectives within this analysis was to ascertain which algorithm allows for maximum power transfer while simultaneously tracking the MPP. The secondary objective was to validate how the MPC controller adapts to the behaviors of the test scenarios in relation to the MPPT algorithms. To determine the maximum energy transfer, we employed the trapezoidal integral (42). In this data context, time *vs.* power was used. The trapezoidal integral was utilized to estimate the total energy contained within a signal, as shown in Eq. (34).

$$\text{Trapezoidal Integral} = \frac{h}{2} \sum_{i=1}^{n} \left(y_{(i-1)} + y_{(i)} \right) \tag{34}$$

Here, (h) is the difference in the time interval value, (n) is the number of intervals, and $(y_{(i-1)})$ and $(y_{(i)})$ are the power values at consecutive points. It should be noted that the maximum power extracted from the system is derived from the area under the curve of the power generated by the PV panel, in comparison with that obtained by each algorithm.

Table **III** presents the results obtained by the algorithms for the critical irradiance test scenario. This includes the area under the curve achieved by implementing the trapezoidal integral and the maximum percentage of energy extracted.

In this analysis, consolidated results are presented for the various optimization algorithms in comparison with the P&O algorithm. All algorithms under review successfully extract power from a PV panel under varying irradiance levels.

This study found that the PSO algorithm achieved the highest power extraction, with a performance of 95.937 % relative to the PV panel power. Fig. **8** illustrates the reference and calculated voltages, as well

Table III. Results obtained with algorithms based on the MPC controller under a scenario of variable average irradiance (critical)

Area under the power curve				
PV panel	**P&O**	**PSO**	**SSA**	**VSA**
56.355	43.594	54.065	53.597	53.716
Percentage of power extracted				
PV panel	**P&O**	**PSO**	**SSA**	**VSA**
100	85.101	95.937	95 .106	95.317

as reference and extracted power for PSO. VSA algorithm followed with 95.317 % power extraction (Fig. **9**). Both algorithms, with their iterative processes and particles, exhibit optimal MPPT responses when tuned under identical conditions. SSA ranked third with 95.106 % extraction, as displayed in Fig. **10**. Lastly, P&O achieved 85.101 %, with Figure **11** showing significant variations in voltage and power due to the algorithm's inherent behavior.

These results were obtained under varying irradiance conditions over time. To determine the algorithm with the highest power extraction, the system was simulated under critical irradiance variations, representing an average 24-hour day compressed into 2.4 seconds in Matlab/Simulink, with each 0.1 second corresponding to an hour of operation.

It should be clarified that, at the beginning of the simulation, the PV array operates under zero solar irradiation, according to the selected irradiation profile. Under this condition, the PV system naturally exhibits the open-circuit voltage when no power conversion is active. However, since the MPPT algorithm imposes a voltage reference associated with the expected MPP, the PV array is unable to sustain this voltage due to energy unavailability. Consequently, the PV voltage decreases and tends toward zero until the solar irradiance level increases.

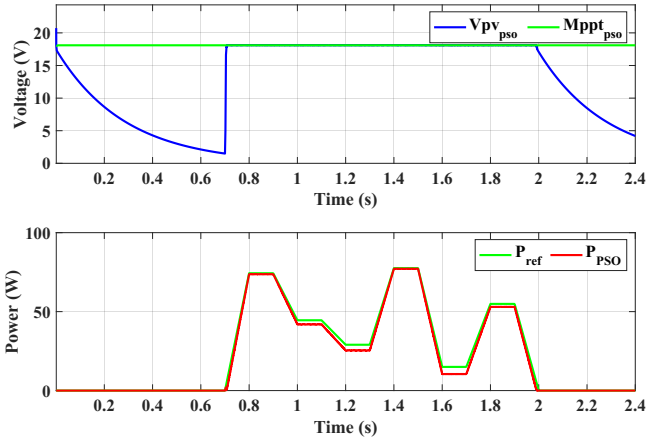

Figure 8. Variation in power demand and generation under average daily irradiance, as determined by the PSO

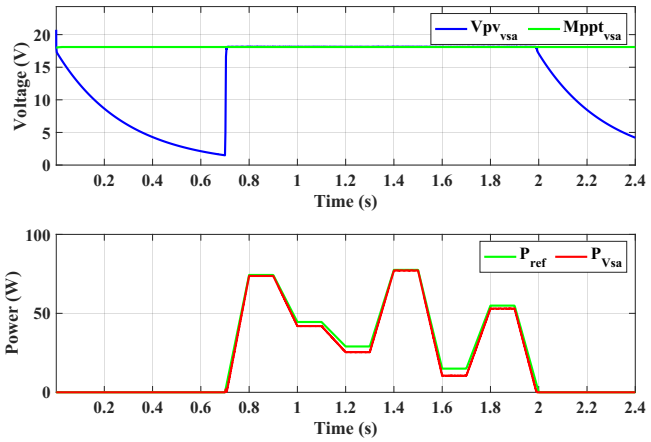

Figure 9. Variation in power demand and generation under average daily irradiance, as determined by the VSA

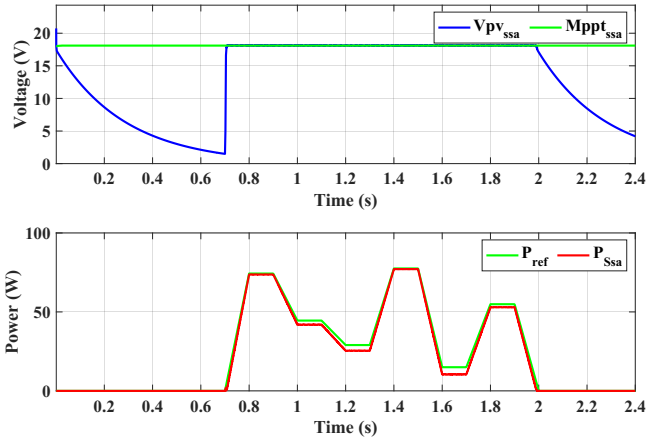

Figure 10. Variation in power demand and generation under average daily irradiance, as determined by the SSA

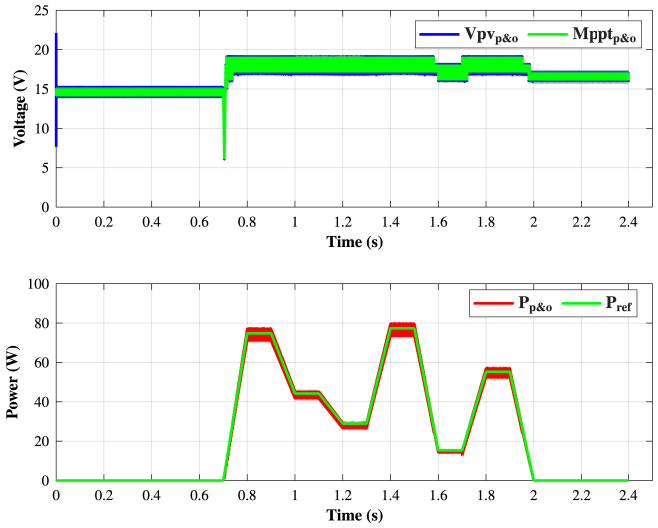

Figure 11. Variation in power demand and generation under average daily irradiance, as determined by the P&O algorithm

4.4. Tests under mean operating conditions

On the other hand, for an average scenario (Table **IV**), the results are presented in the same manner as in Table **III**. Here, under an average irradiance curve, note how the algorithms manage to extract maximum power.

Table IV. Results obtained with algorithms based on the MPC controller under a scenario of average irradiance

Area under the power curve				
PV panel	**P&O**	**PSO**	**SSA**	**VSA**
56	42.671	52.941	52 .706	52.762
Percentage of power extracted				
PV panel	**P&O**	**PSO**	**SSA**	**VSA**
100	84.056	94.538	94 .118	94.218

To validate the test systems, an average daily irradiance condition was applied. According to the results, the PSO algorithm achieved the highest power extraction, with 94.538 % relative to PV panel power, as shown in Fig, **12** alongside the corresponding voltage variations. The VSA followed with 94.218 % power extraction (Fig. **13**). In third place, SSA achieved 94.118 %, exhibiting a similar behavior to other optimization algorithms (Fig. **14**). Finally, P&O reached 84.056 %, with Figure **15** highlighting pronounced variations in voltage and power due to its nature.

During the simulation of these systems, various tests were conducted under different irradiance levels over a test period of 2.4 s. This allowed observing the way in which optimization algorithms are capable of extracting more power in response to system changes under any irradiance profile compared

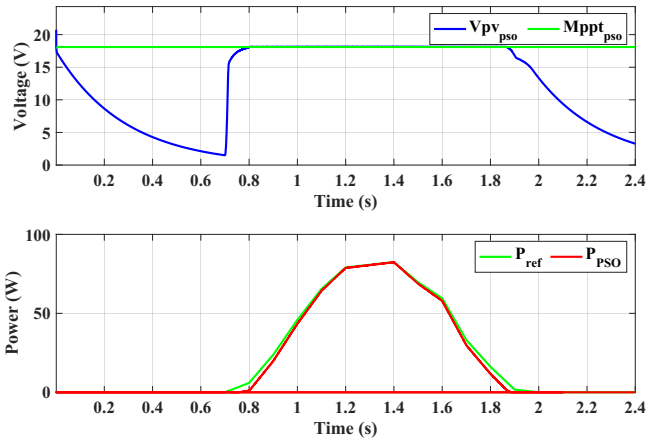

Figure 12. Variation in power demand and generation under critical daily irradiance, as determined by the PSO

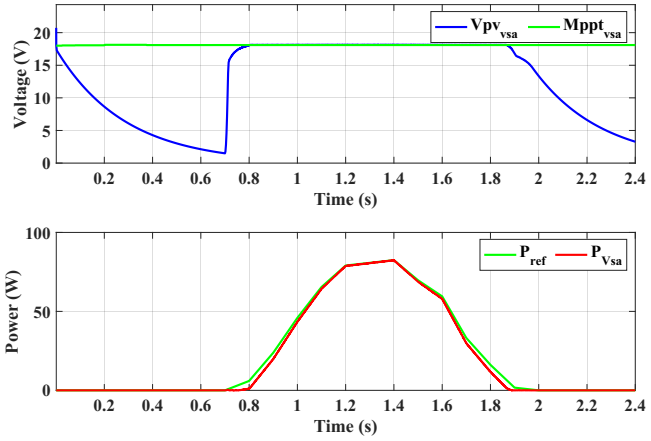

Figure 13. Variation in power demand and generation under critical daily irradiance, as determined by the VSA

to P&O. It was evident that the algorithm that enables maximum power extraction is PSO. In the critical scenario, an average power of 91.615 % was obtained by the algorithms, and, on an average day, 91.733 % of the power was extracted.

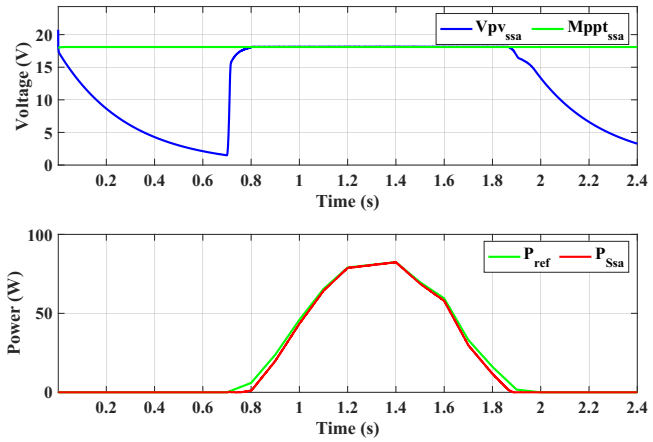

Figure 14. Variation in power demand and generation under critical daily irradiance, as determined by the SSA

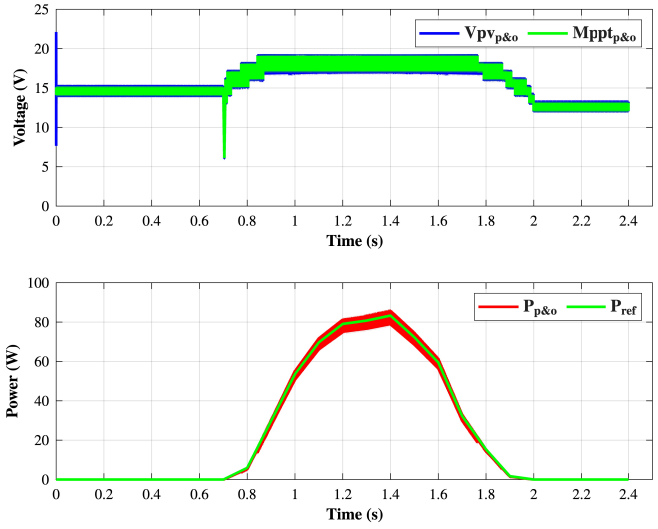

Figure 15. Variation in power demand and generation under critical daily irradiance, as determined by the P&O algorithm

5. Conclusions

This study presented a comprehensive analysis of four MPPT algorithms, *i.e.*, P&O, PSO, SSA, and VSA, focused on maximizing power extraction from a PV panel. Emphasis was placed on the objective function and algorithm efficiency under varying irradiance levels, including both average daily and critical conditions. Using Matlab/Simulink, complex scenarios that reflect real-world PV configurations were simulated. The analysis used a trapezoidal integral to evaluate the area under the power curve, showing that PSO achieved approximately 95.937 % and 94.538 % of power extraction under critical and average conditions, respectively. The remaining algorithms followed in order: VSA, SSA, and

P&O. Visual representations further illustrated system responses, providing a clearer understanding of voltage-power relationships. Given its high efficiency, PSO emerges as a strong candidate for future PV system applications, particularly in scenarios with partial and total shading. Additionally, the MPC controller demonstrated adaptability, effectively adjusting the boost DC/DC converter to maintain MPPT under variable irradiance conditions. This adaptability highlights MPC's potential for future PV implementations that encounter fluctuating environmental conditions. Future work aims to develop a DMPPT platform to support series-connected PV systems. This would include integrating monitoring systems with energy storage, enabling optimal management and stability under conditions with varying irradiance and improving system efficiency for different PV applications.

6. Author contributions

Conceptualization: Jhon Anderson Gómez Pemberty, Jaime Alberto Ramírez Ospina.
Methodology: Jose Mena, Juan Esteban Zabala.
Software: Jose Mena, Jhon Anderson Gómez Pemberty.
Validation: Jose Mena, Juan Esteban Zabala.
Formal analysis: Jose Mena, Jhon Anderson Gómez Pemberty.
Investigation: Jose Mena, Jhon Anderson Gómez Pemberty.
Resources: Juan Esteban Zabala.
Data curation: Jose Mena.
Writing – original draft: Jose Mena.
Writing – review and editing: Jose Mena, Juan Esteban Zabala.
Visualization: Jose Mena.
Supervision: Juan Esteban Zabala, Jaime Alberto Ramírez Ospina.
Project administration: Jhon Anderson Gómez Pemberty.
Funding acquisition: Institución Universitaria Digital de Antioquia.

7. Conflicts of Interest

The authors declare no conflicts of interest.

8. Declaration of generative AI and AI-assisted technologies in the writing process

During the preparation of this work, the authors used ChatGPT to improve the writing. After using this tool, the authors reviewed and edited the content as needed and take full responsibility for the content of this publication.

References

[1] T. Ahmad and D. Zhang, "A critical review of comparative global historical energy consumption and future demand: the story told so far," *Energy Rep.*, vol. 6, pp. 1973–1991, 2020.

[2] K. Makieła, B. Mazur, and J. Głowacki, "The impact of renewable energy supply on economic growth and productivity," *Energies*, vol. 15, no. 13, p. 4808, 2022.

[3] Y. Zhu and C. Huo, "The impact of agricultural production efficiency on agricultural carbon emissions in china," *Energies*, vol. 15, no. 12, p. 4464, 2022.

[4] M. Khezri, M. S. Karimi, J. Mamkhezri, R. Ghazal, and L. Blank, "Assessing the impact of selected determinants on renewable energy sources in the electricity mix: the case of ASEAN countries," *Energies*, vol. 15, no. 13, p. 4604, 2022.

[5] P. Zhang and D. Hao, "Enterprise financial management and fossil fuel energy efficiency for green economic growth," *Resour. Policy*, vol. 84, p. 103763, 2023.

[6] C. Tudor and R. Sova, "On the impact of GDP per capita, carbon intensity and innovation for renewable energy consumption: worldwide evidence," *Energies*, vol. 14, no. 19, p. 6254, 2021.

[7] A. Bughneda, M. Salem, A. Richelli, D. Ishak, and S. Alatai, "Review of multilevel inverters for PV energy system applications," *Energies*, vol. 14, no. 6, p. 1585, 2021.

[8] I. Jagadeesh and V. Indragandhi, "Comparative study of DC-DC converters for solar PV with microgrid applications," *Energies*, vol. 15, no. 20, p. 7569, 2022.

[9] M.-H. Hwang, Y.-G. Kim, H.-S. Lee, Y.-D. Kim, and H.-R. Cha, "A study on the improvement of efficiency by detection solar module faults in deteriorated photovoltaic power plants," *Appl. Sci.*, vol. 11, no. 2, p. 727, 2021.

[10] S. A. Gorji, H. G. Sahebi, M. Ektesabi, and A. B. Rad, "Topologies and control schemes of bidirectional DC–DC power converters: an overview," *IEEE Access*, vol. 7, pp. 117 997–118 019, 2019.

[11] L. Zhang, Z. Wang, S. Li, S. Ding, and H. Du, "Universal finite-time observer based second-order sliding mode control for DC-DC buck converters with only output voltage measurement," *J. Franklin Inst.*, vol. 357, no. 16, pp. 11 863–11 879, 2020.

[12] M. Mao, L. Cui, Q. Zhang, K. Guo, L. Zhou, and H. Huang, "Classification and summarization of solar photovoltaic MPPT techniques: a review based on traditional and intelligent control strategies," *Energy Rep.*, vol. 6, pp. 1312–1327, 2020.

[13] R. B. Bollipo, S. Mikkili, and P. K. Bonthagorla, "Hybrid, optimal, intelligent and classical PV MPPT techniques: a review," *CSEE J. Power Energy Syst.*, vol. 7, no. 1, pp. 9–33, 2020.

[14] S. Bhattacharyya, D. S. P. Kumar, S. Samanta, and S. Mishra, "Steady output and fast tracking MPPT (SOFT-MPPT) for P&O and InC algorithms," *IEEE Trans. Sustain. Energy*, vol. 12, no. 1, pp. 293–302, 2021.

[15] P. Kumar and I. Srikanth, "Power quality performance enhancement by PV-based distribution static compensator under incremental conductance maximum power point tracking algorithm," *Cleaner Energy Syst.*, vol. 4, p. 100062, 2023.

[16] F. J. Diez, A. Martínez-Rodríguez, L. M. Navas-Gracia, L. Chico-Santamarta, A. Correa-Guimaraes, and R. Andara, "Estimation of the hourly global solar irradiation on the tilted and oriented plane of photovoltaic solar panels applied to greenhouse production," *Agronomy*, vol. 11, no. 3, p. 495, 2021.

[17] J. A. Qahouq, Y. Jiang, and W. Huang, "Load-voltage-based single-sensor MPPT controller for multi-channel PV systems," in *Proc. IEEE Appl. Power Electron. Conf. Expo. (APEC)*, 2014, pp. 3451–3454.

[18] A. Ortiz, E. Mendez, I. Macias, and A. Molina, "Earthquake algorithm-based voltage referenced MPPT implementation through a standardized validation frame," *Energies*, vol. 15, no. 23, p. 8971, 2022.

[19] M. Jiang, M. Ghahremani, S. Dadfar, H. Chi, Y. N. Abdallah, and N. Furukawa, "A novel combinatorial hybrid SFL–PS algorithm based neural network with perturb and observe for the MPPT controller of a hybrid PV-storage system," *Control Eng. Pract.*, vol. 114, p. 104880, 2021.

[20] S. Hadji, J.-P. Gaubert, and F. Krim, "Real-time genetic algorithms-based MPPT: study and comparison (theoretical and experimental) with conventional methods," *Energies*, vol. 11, no. 2, p. 459, 2018.

[21] M. H. Zafar, N. M. Khan, A. F. Mirza, and M. Mansoor, "Bio-inspired optimization algorithms based maximum power point tracking technique for photovoltaic systems under partial shading and complex partial shading conditions," *J. Cleaner Prod.*, vol. 309, p. 127279, 2021.

[22] R. Mas, A. Berastain, A. Antoniou, L. Angeles, S. Valencia, and C. Celis, "Genetic algorithms-based size optimization of directly and indirectly coupled photovoltaic-electrolyzer systems," *Energy Convers. Manag.*, vol. 270, p. 116213, 2022.

[23] A. G. Abo-Khalil, I. I. El-Sharkawy, A. Radwan, and S. Memon, "Influence of a hybrid MPPT technique, SA-P&O, on PV system performance under partial shading conditions," *Energies*, vol. 16, no. 2, p. 577, 2023.

[24] M. A. Hafeez, A. Naeem, M. Akram, M. Y. Javed, A. B. Asghar, and Y. Wang, "A novel hybrid MPPT technique based on harris hawk optimization (HHO) and perturb and observer (P&O) under partial and complex partial shading conditions," *Energies*, vol. 15, no. 15, p. 5550, 2022.

[25] M. Rastogi, A. Ahmad, and A. H. Bhat, "Performance investigation of two-level reduced-switch D-STATCOM in grid-tied solar-PV array with stepped P&O MPPT algorithm and modified SRF strategy," *J. King Saud Univ. Eng. Sci.*, 2021.

[26] K. Ali, L. Khan, Q. Khan, S. Ullah, S. Ahmad, S. Mumtaz, F. W. Karam, and Naghmash, "Robust integral backstepping based nonlinear MPPT control for a PV system," *Energies*, vol. 12, no. 16, p. 3180, 2019.

[27] S. Mo, Q. Ye, K. Jiang, X. Mo, and G. Shen, "An improved MPPT method for photovoltaic systems based on mayfly optimization algorithm," *Energy Rep.*, vol. 8, pp. 141–150, 2022.

[28] T. Hai, J. Zhou, and K. Muranaka, "An efficient fuzzy-logic based MPPT controller for grid-connected PV systems by farmland fertility optimization algorithm," *Optik*, vol. 267, p. 169636, 2022.

[29] B. C. Phan, Y.-C. Lai, and C. E. Lin, "A deep reinforcement learning-based MPPT control for PV systems under partial shading condition," *Sensors*, vol. 20, no. 11, p. 3039, 2020.

[30] M. L. Katche, A. B. Makokha, S. O. Zachary, and M. S. Adaramola, "A comprehensive review of maximum power point tracking (MPPT) techniques used in solar PV systems," *Energies*, vol. 16, no. 5, p. 2206, 2023.

[31] A. Almutairi, A. G. Abo-Khalil, K. Sayed, and N. Albagami, "MPPT for a PV grid-connected system to improve efficiency under partial shading conditions," *Sustainability*, vol. 12, no. 24, p. 10310, 2020.

[32] S. Angadi, U. R. Yaragatti, Y. Suresh, and A. B. Raju, "System parameter based performance optimization of solar PV systems with perturbation based MPPT algorithms," *Energies*, vol. 14, no. 7, p. 2007, 2021.

[33] A. Gündoğdu, "System identification based ARV-MPPT technique for PV systems under variable atmospheric conditions," *IEEE Access*, vol. 10, pp. 51 325–51 342, 2022.

[34] L. Tightiz, S. Mansouri, F. Zishan, J. Yoo, and N. Shafaghatian, "Maximum power point tracking for photovoltaic systems operating under partially shaded conditions using SALP swarm algorithm," *Energies*, vol. 15, no. 21, p. 8210, 2022.

[35] Z.-K. Fan, A. Setianingrum, K.-L. Lian, and S. Suwarno, "A hybrid approach for photovoltaic maximum power tracking under partial shading using honey badger and genetic algorithms," *Energies*, vol. 17, no. 16, p. 3935, 2024.

[36] L. A. T. Grisales, C. A. Ramos-Paja, and A. J. Saavedra-Montes, "Techniques for modeling photovoltaic systems under partial shading," *Tecnura*, vol. 20, no. 48, pp. 171–183, 2016.

[37] A. Gómez and R. Correa, "Implementación de un sistema de control predictivo multivariable en un horno," *Dyna*, vol. 76, no. 157, pp. 195–203, 2009.

[38] MathWorks, "Model predictive control toolbox," 2023, https://la.mathworks.com/products/model-predictive-control.html (accessed Jun. 21, 2023). [Online]. Available: https://la.mathworks.com/products/model-predictive-control.html

[39] J. Kennedy and R. Eberhart, "Particle swarm optimization," in *Proc. IEEE Int. Conf. Neural Netw. (ICNN)*, vol. 4, 1995, pp. 1942–1948.

[40] B. Doğan and T. Ölmez, "A new metaheuristic for numerical function optimization: vortex search algorithm," *Inf. Sci.*, vol. 293, pp. 125–145, 2015.

[41] J. Montano, A. F. T. Mejia, A. A. R. Muñoz, F. Andrade, O. D. G. Rivera, and J. M. Palomeque, "Salp swarm optimization algorithm for estimating the parameters of photovoltaic panels based on the three-diode model," *Electronics*, vol. 10, no. 24, p. 3123, 2021.

[42] S. S. Dragomir, P. Cerone, and A. Sofo, "Some remarks on the trapezoid rule in numerical integration," *RGMIA Res. Rep. Collect.*, vol. 2, no. 5, 1999.

Jose Mena

from Medellín, Antioquia, Colombia, earned his Bachelor's degree in Mechatronics Engineering from Instituto Tecnológico Metropolitano (ITM) in 2017. He is currently pursuing a Master's degree in

Automation and Industrial Control at ITM and works as a lecturer in the Department of Mechatronics at Institución Universitaria Digital de Antioquia. His research interests include renewable energy systems, power electronics, smart grids, photovoltaic systems optimization, fault diagnosis in photovoltaic panels, intelligent energy storage management, prototyping, microelectronics, and embedded systems.
Email: jose.mena@prof.iudigital.edu.co

Juan Esteban Zabala-Daza

from Medellín, Antioquia, Colombia, earned his Bachelor's degree in Mechatronics Engineering from Instituto Tecnológico Metropolitano (ITM). He is currently a researcher focused on control systems and photovoltaic energy applications. His research interests include model-predictive control, optimization algorithms, renewable energy systems, and advanced control strategies applied to power electronics.
Email: juan.zabala@itm.edu.co

Jhon A. Gómez P.

from Medellín, Antioquia, Colombia, earned his Bachelor's degree in Mechatronic Engineering from Instituto Tecnológico Metropolitano (ITM) in 2017. He earned a Specialist's degree in Project Formulation and Evaluation at Institución Universitaria Digital de Antioquia. His research interests include renewable energy systems, power electronics, photovoltaic systems optimization, fault diagnosis in electronic systems, prototyping, microelectronics, PLC programming, and embedded systems.
Email: jhon.gomez95@est.iudigital.edu.co

Jaime A. Ramírez-Ospina

from Itagüí, Antioquia, Colombia, earned his Bachelor's degree in Instrumentation and Control Engineering from Politécnico Jaime Isaza Cadavid in 2013. He has professional experience in industrial automation and is currently pursuing a Master's degree in Innovation and Technology at Universidad El Bosque. He also works as a lecturer in the Department of Mechatronics at Institución Universitaria Digital de Antioquia. His research interests include industrial automation, industrial process optimization, renewable energy systems, photovoltaic systems optimization, intelligent energy storage management, and educational innovation in engineering.
Email: jaime.ramirez@iudigital.edu.co